Journal of Biomechanics 44 (2011) 2299–2306

Contents lists available at ScienceDirect

Journal of Biomechanics

journal homepage: www.elsevier.com/locate/jbiomech
www.JBiomech.com

Contractile and non-contractile tissue volume and distribution in ankle muscles of young and older adults

Christopher J. Hasson [a,*], Jane A. Kent-Braun [b], Graham E. Caldwell [a]

[a] Biomechanics Laboratory, Department of Kinesiology, University of Massachusetts Amherst, USA
[b] Muscle Physiology Laboratory, Department of Kinesiology, University of Massachusetts Amherst, USA

ARTICLE INFO

Article history:
Accepted 26 May 2011

Keywords:
Dorsiflexor
Plantar flexor
Volume
Aging
MRI
Contractile tissue
Non-contractile tissue

ABSTRACT

Magnetic resonance imaging (MRI) enables accurate *in vivo* quantification of human muscle volumes, which can be used to estimate subject-specific muscle force capabilities. An important consideration is the amount of contractile and non-contractile tissue in the muscle compartment, which will influence force capability. We quantified age-related differences in the proportion and distribution of contractile and non-contractile tissue in the dorsiflexor and plantar flexor (soleus, and medial and lateral heads of gastrocnemius) muscles, and examined how well these volumes can be estimated from single MRI cross-sections. Axial MRIs of the left leg for 12 young (mean age 27 years) and 12 older (72 years) healthy, active adults were used to compute muscle volumes. Contractile tissue distribution along the leg was characterized by mathematical functions to allow volume prediction from single-slice cross-sectional area (CSA) measurements. Compared to young, older adults had less contractile volume and a greater proportion of non-contractile tissue. In both age groups the proportion of non-contractile tissue increased distally, with the smallest proportion near the maximum compartment CSA. A single CSA measurement predicted contractile volume with 8–11% error, with older adults in the higher end of this range. Using multiple slices improved volume estimates by roughly 50%, with average errors of about 3–4%. These results demonstrate significant age-related differences in non-contractile tissue for the dorsi- and plantar-flexor muscles. Although estimates of contractile volume can be obtained from single CSA measurements, multiple slices are needed for increased accuracy due to inter-individual variations in muscle volume and composition.

1. Introduction

In modeling the musculoskeletal system, researchers typically scale muscular parameters to that of an average young male (Kuo and Zajac, 1993; van Soest and Bobbert, 1993; Anderson and Pandy, 2001), despite large variation in muscle morphology and physiology between subjects (Lexell and Taylor, 1989). Failure to account for these subject-specific differences can compromise the accuracy of musculoskeletal models (Scovil and Ronsky, 2006).

An important parameter for individual muscles is maximal isometric force (P_0), which cannot be measured experimentally due to the redundancy of the musculoskeletal system (Yamaguchi et al., 1995). An alternative is to estimate P_0 from individual muscle volumes (Caldwell and Chapman, 1991), which can be measured accurately and reliably *in vivo* using magnetic resonance imaging (MRI) (Mitsiopoulos et al., 1998).

A contiguous series of axial MR images is considered the gold standard for muscle volume measurement (Narici et al., 1992), although this requires significant analysis time (Mitsiopoulos et al., 1998). However, Morse et al. (2007) calculated quadriceps volume in young adults from a single axial MRI image, thereby reducing analysis time considerably. They reported an error of ~10% compared to a full image set, but it is unclear how well a single scan will work for muscles with different morphologies and populations such as the elderly. Many older adults have sarcopenia, a prominent reduction in contractile tissue (Roubenoff and Hughes, 2000). Concomitantly with increased age, there is a two- to six-fold muscle-specific increase in the percentage of non-contractile tissue (Forsberg et al., 1991; Overend et al., 1992; Jubrias et al., 1997; Kent-Braun et al., 2000). However, these studies have assessed non-contractile tissue at only a few locations, so little is known about non-contractile tissue distribution. Age-related changes in the proportion and/or distribution of contractile and non-contractile tissue will affect volume estimates from single images, but the size of this effect is currently unknown.

Therefore, the aims of this study were to quantify the volume, proportion, and longitudinal distribution of contractile and non-contractile volumes in the dorsiflexor and plantar flexor muscles

* Corresponding author. Current address: Department of Biology, 134 Mugar Life Science Building, Northeastern University, 360 Huntington Avenue, Boston MA 02115-5005, USA. Tel.: +1 617 373 7070; fax: +1 617 373 3724.
E-mail address: cjhasson@neu.edu (C.J. Hasson).

0021-9290/$ - see front matter © 2011 Elsevier Ltd. All rights reserved.
doi:10.1016/j.jbiomech.2011.05.031

of young and older adults, and to determine whether contractile volumes can be accurately estimated in both groups from single MRI cross-sections and models of tissue distribution.

2. Methods

2.1. Subjects

Twelve young (21–31 yrs) and 12 older (66–79 yrs) male and female subjects, free from musculoskeletal or neurological impairments, participated in the study (Table 1). The young subjects were a typical population of graduate students who all participated in regular physical activity. The older subjects were independent, community-dwelling adults who engaged in regular physical activity, typically walking for exercise several times a week. Prior to participating, subjects read and signed an informed consent document approved by the university's institutional review board.

2.2. Magnetic resonance imaging

Image acquisition: axial images ("slices") of the left leg were taken using a 1.5 T MRI system (Sigma EchoSpeed Plus, General Electric) with a phased-array coil, using standard imaging parameters: T_1-weighted spin echo sequence, 4 mm slice thickness with no gap, 400 ms repetition time, 11 ms echo time, 512×512 pixel resolution, 30 cm field of view. Due to leg length variation, the number of slices ranged from 114 to 171 (*mean*=139), with total acquisition time ranging from ~20–30 min.

Muscle cross-sectional areas: adapting our earlier approach (Kent-Braun et al., 2000), a MATLAB™ (Mathworks, Natick MA) program was created to identify muscle cross-sectional area (CSA) and to separate contractile and non-contractile tissue. Two observers outlined the perimeters of the soleus (SO), lateral (GL), and medial (GM) heads of the gastrocnemius, and the combined DF muscles (tibialis anterior, extensor hallucis longus, extensor digitorum longus, and peroneus tertius) in every other slice (Fig. 1), giving an effective image spacing of 8 mm. Observer A outlined 15 subjects and Observer B 9 subjects, using MR images from the Visible Human male dataset (Ackerman, 1991) as a guide.

Table 1
Subject characteristics (mean ± standard deviation).

Group[a]		*n*	Age (yrs)	Ht. (cm)	Mass (kg)[†]	L_{Leg} (cm)	BMI[b†]	DF T_0 (Nm)[c†]	PF T_0 (Nm)[c†]
Y	M	6	27 ± 3	181 ± 6	76.9 ± 8.2	24.9 ± 3.0	24.9 ± 3.0	42 ± 9	114 ± 28
	F	6	26 ± 3	165 ± 8	57.2 ± 6.6	21.9 ± 1.1	21.9 ± 1.1	31 ± 7	71 ± 23
O	M	6	73 ± 5	177 ± 8	91.7 ± 10.3	30.1 ± 2.0	30.1 ± 2.0	35 ± 7	61 ± 10
	F	6	70 ± 5	166 ± 9	72.6 ± 17.0	26.7 ± 3.4	26.7 ± 3.4	34 ± 12	79 ± 34

[a] Y: young; O: older; M: male; F: female.
[b] BMI: body mass index: mass (kg) divided by squared height (m).
[c] Maximal isometric torque (T_0) for dorsiflexors (DFs) and plantar flexors (PFs), measured with a Biodex dynamometer. Note that these measures were taken with the knee bent at 90°; also the relatively high torque values for the older females are skewed by two particularly strong subjects.
[†] For mass: main effects of age ($p<.001$; $F=15.0$) and gender ($p<.001$; $F=40.0$); for BMI: main effects of age ($p<.001$; $F=25.7$) and gender ($p=.003$; $F=11.5$); for T_0, main effect of age ($p=.028$; $F=5.2$) and three way-interaction between age, gender, and muscle group ($p=.034$; $F=4.8$). *n*: number of subjects; L_{Leg}: leg length.

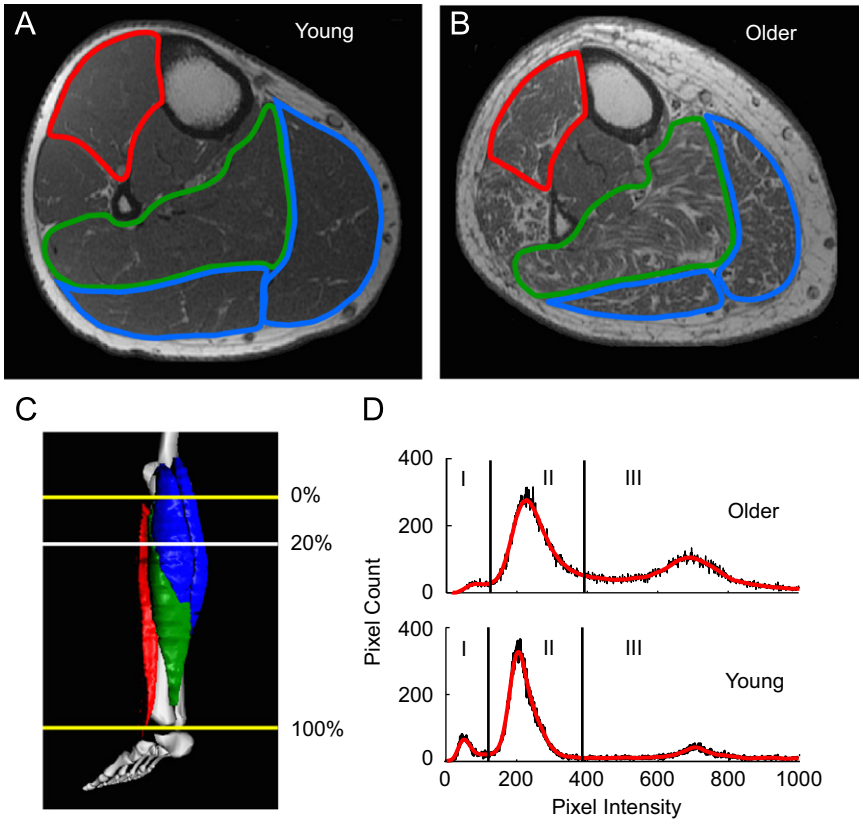

Fig. 1. Comparison of axial MRI slices from one young (A; aged 29 years) and one older (B; aged 79 years) male at 20% leg length (C). Note significant increase in non-contractile tissue (light pixel intensities) in the older subject. Muscles are color-coded: dorsiflexors=red; soleus=green; gastrocnemius=blue. Panel (D) shows example young and old pixel intensity histograms separating tissue into cortical bone and connective tissue (I), muscle (II), and trabecular bone and adipose tissue (III). Both raw (black) and smoothed (red) data are shown. (For interpretation of the references to color in this figure legend, the reader is referred to the web version of this article.)

Tissue separation: to quantify contractile and non-contractile content for each muscle, the analysis software generated a histogram of the intensity distribution for all pixels within the anatomical segment boundary for each slice (Fig. 1D). Lower intensities represent cortical bone and connective tissue, higher intensities represent trabecular bone and adipose tissue, and intermediate intensities represent muscle tissue (Kent-Braun et al., 2000; Gomberg et al., 2005). Separation thresholds were automatically chosen as the intensities at zero slope on either side of the peak muscle intensity, after applying a 40-point moving average smoothing function to the histogram data. Pixels were re-colored on the images based on these thresholds to facilitate small adjustments by the user to the automated thresholds.

CSA computation: total CSA (CSA_T) was calculated by multiplying the number of pixels within an outlined region by single pixel area. Contractile-only CSA (CSA_C) was similarly calculated, with the pixel count limited to intermediate intensities. Non-contractile tissue CSA (CSA_{NC}) was calculated as $CSA_T - CSA_C$.

2.3. Analysis

Reliability: to assess intra-observer reliability, Observer A re-analyzed the slices at 20% and 40% leg length of all 15 subjects several months later in a blinded fashion. To assess inter-rater reliability, Observer A also re-analyzed the 20% and 40% slices of Observer B's 9 subjects.

Muscle volume calculations from MRI dataset: for each subject, a five-point moving average was used to remove high-frequency measurement noise in the CSA data, applied to each muscle for the entire set of contiguous scans along its length. Because this measurement noise is random, the smoothing does not affect the volume measures. Total (V_T) and contractile-only (V_C) muscle volumes were computed by trapezoidal integration of the CSA_T and CSA_C curves, respectively

$$V = \int_p^d \mathrm{CSA}\,dx \approx \sum_{i=p}^{d-1} \Delta x(\mathrm{CSA}_i + \mathrm{CSA}_{i+1})/2 \quad (1)$$

where V is the volume (either V_T or V_C), p and d are the slice numbers (i) of the most proximal and distal images containing muscle tissue, respectively, and the step size (Δx) is 8 mm. Non-contractile tissue volume, V_{NC}, was calculated as $V_T - V_C$, and expressed as a percentage of the total muscle volume ($V_{\%NC}$).

Characterization of CSA distribution: each subject's CSA data were normalized to lower leg length L_{Leg}, determined from axial images in which the tibial plateau and lateral malleolus apex were visible. Slices were linearly interpolated to integer percentages of this distance (knee: 0%; ankle: 100%). For each muscle, the longitudinal distribution of non-contractile tissue along the leg was assessed by computing CSA_{NC} relative to CSA_T. This distribution was averaged across subjects within each age group, and modeled with best-fit second-order polynomials.

The DF and PF longitudinal CSA_C distributions as a function of L_{Leg} were characterized by four-parameter generalized extreme value (GEV) distributions (Kotz and Nadarajah, 2000). For each subject and muscle, the CSA_C from each image was divided by the maximum CSA_C for that muscle (CSA_{Max}), giving a normalized CSA_N (i.e. $CSA_N = CSA_C/CSA_{Max}$). CSA_N was averaged within the age groups and fitted with GEV distributions using a non-linear least squares approach; the GEV distributions were given by the formula

$$\mathrm{CSA}_N = a(1/\sigma)(1+\xi z)^{(-1/\xi)-1}\exp\left[-(1+\xi z)^{-1/\xi}\right] \quad (2)$$

where $z=(SL-\mu)/\sigma$. Parameters μ and σ translate and scale the function, respectively, along the x-axis (longitudinal slice location), ξ changes the shape of the function, and a scales the function along the y-axis (CSA_N). SL is the slice location as a percentage of L_{Leg}. Eq. (2) yields a CSA_N at any given SL between p and d.

Predicting muscle volumes from single MRI scans: for each subject, a nominal contractile volume (V_N) was calculated for each muscle by analytically integrating Eq. (2) on the interval from p to d, giving

$$V_N = a\exp\left[\left(\frac{\sigma+d\xi-\xi\mu}{\sigma}\right)^{-1/\xi}\right]^{-1} - a\exp\left[\left(\frac{\sigma+p\xi-\xi\mu}{\sigma}\right)^{-1/\xi}\right]^{-1} \quad (3)$$

where p and d are expressed as a percentage of L_{Leg}. The predicted contractile volume $\tilde{V}_C$ (cm^3) is given by

$$\tilde{V}_C = V_N \mathrm{CSA}_{Max} L_{Leg}/100 \quad (4)$$

Given the GEV coefficients (μ, σ, ξ, a) and integration limits (p, d), subject-specific contractile volumes can be estimated for a muscle by calculating V_N using Eq. (3), and then solving Eq. (4) for $\tilde{V}_C(cm^3)$ using a single CSA_{Max} (cm^2) measurement at a known L_{Leg} (cm) (Morse et al., 2007). Finding the true CSA_{Max} experimentally may require many scans; an alternative is to estimate CSA_{Max} from a non-maximal CSA_C measurement at a given SL, using Eq. (2) to solve for CSA_N, where $CSA_{Max} = CSA_C/CSA_N$.

For each subject $\tilde{V}_C$ was predicted using the GEV coefficients and integration limits (p, d) specific to that subject's age group, as well as a generic set of GEV coefficients (average of both age groups). Several estimation options were explored. First, $\tilde{V}_C$ was estimated using CSA_C from a single image located at 30% L_{Leg} for all muscles. The second estimate used images close to CSA_{Max} for each muscle, drawn from slices at 40% L_{Leg} (DF, SO) and 20% L_{Leg} (GL, GM). One drawback is that measurement error in these single slices could result in poor volume estimates. If more slices are used this error should be reduced, so CSA_{Max} was also computed based on an *average* CSA_{Max} calculated from three, five, or ten slices per muscle.

2.4. Statistics

Intra- and inter-observer reliability was quantified with the intra-class correlation coefficient (ICC) (Shrout and Fleiss, 1979) and the standard error of the mean (SEM) (Harvill, 1991), using the approach of Weir (2005). To test for intra- and inter-observer bias, a repeated-measures ANOVA was performed with observer and subject as random factors (significance at $p<.1$). Linear mixed-effects models were used to assess differences in absolute muscle volumes, with age, gender, muscle, and volume type (V_T or V_C) as fixed factors, and subject as a random factor (significance at $p<.05$). While gender differences were expected for these absolute measures, there was no *a priori* expectation for the relative measure $V_{\%NC}$. Therefore, within each age group $V_{\%NC}$ data were pooled across the genders before completing a separate mixed model analysis. Mixed-model-based t-tests ($p<.05$) were used for pairwise comparisons using a Bonferoni correction. Coefficients of determination (r^2) were used to assess the goodness of fit between non-contractile tissue distributions (CSA_{NC}/CSA_T) and polynomial fits, and between measured contractile volumes (V_C) and GEV model predictions ($\tilde{V}_C$). Linear regressions between V_C and $\tilde{V}_C$ were performed for each subject; fits were evaluated using the variance explained (r^2) and the standard error of estimate (SEE). A Bland–Altman analysis was performed to quantify bias and limits of agreement for the volume predictions (Bland and Altman, 1986).

3. Results

Older subjects had greater mass and a greater body mass index (Table 1). Visual inspection of the images revealed considerably more non-contractile tissue in the older subjects (Fig. 1), with most non-contractile tissue uniformly distributed across each axial slice. Only one subject had distinct fatty inclusions in the PF muscles.

CSA reliability: ICCs were above .90 for intra- and inter-observer reliability (Supplementary Material, Table S1) for the four muscles, two slice locations, and two area types (CSA_T, CSA_C). The CSA SEM varied between 1.13 and 14.39 mm^2. There was little systematic over- or under-estimation of CSAs within or between observers, reflected by insignificant ANOVA results ($p>.1$). The exception was for DF at 40% L_{Leg}, in which one observer had a small (4 mm^2; .3%) but consistent overestimation of CSA_T.

Measured muscle volumes: for young subjects there was no difference between total volume V_T and contractile volume V_C (post-hoc single-factor $p=.102$), but older adults had smaller V_C compared to V_T (post-hoc single-factor $p<.001$; Age x volume type interaction $p=.039$; Table 2). Across the four muscles, older adults had on average 3.6 times more non-contractile tissue ($V_{\%NC}$; main effect). Overall, males had larger volumes than females (gender main effect for absolute volume, collapsed across V_T and V_C). Finally, for absolute volume there was a main effect of muscle, such that SO volumes were largest (post-hoc $p<.001$), followed by GM and DF (similar volumes; $p=.640$), and GL was the smallest ($p<.001$).

Characterization of measured CSA distribution: the shapes of the longitudinal CSA_C distributions approximated skewed normal distributions, with DF the most skewed (Fig. 2). Each age group's average CSA_C distribution was well approximated by the GEV model, with the lowest $r^2=.97$ (Table 3). The GL and GM had maximum CSA_C at ~20% L_{Leg}, while DF and SO maximums were more distal, at ~40% of L_{Leg} (Table 3). A non-linear relation for the CSA_{NC}/CSA_T distribution reflected a varying proportion of non-contractile tissue along the length of the leg, with lowest proportions near the center of the muscle belly and a tendency to increase distally, especially in DF and SO (Fig. 3).

Muscle volume predictions: using age-specific equations from a single-slice at 30% L_{Leg}, the strength of the relation between the actual and predicted contractile volumes (r^2) ranged from .77 to .96 for young and .72 to .97 for old, and accuracy (SEE) ranged from 5–11% for young (mean across muscles=8%) and 5–15% for old (mean=11%; Table 4; Fig. 4). The DF consistently had the greatest r^2

Table 2
Muscle volumes. Total (V_T), contractile (V_C), and percent non-contractile ($V_{\%NC}$) tissue volumes for each muscle. Values are mean ± standard deviation.

Group [a]		Variable [†]	Muscle [b]				
			DF	SO	GL	GM	TS [c]
Y	M (n=6)	V_T (cm^3)	275 ± 32	442 ± 61	147 ± 30	264 ± 59	853
		V_C (cm^3)	256 ± 27	423 ± 53	139 ± 28	255 ± 56	817
	F (n=6)	V_T (cm^3)	208 ± 49	408 ± 65	117 ± 12	220 ± 69	745
		V_C (cm^3)	191 ± 44	387 ± 66	110 ± 11	213 ± 69	710
	Pooled (n=12)	$V_{\%NC}$ (%) [d]	4.5 ± 4.0	2.4 ± 2.7	2.9 ± 3.1	1.7 ± 2.0	2.8
O	M (n=6)	V_T (cm^3)	302 ± 53	517 ± 157	135 ± 33	233 ± 32	885
		V_C (cm^3)	257 ± 45	371 ± 151	110 ± 33	189 ± 43	670
	F (n=6)	V_T (cm^3)	206 ± 21	397 ± 53	85 ± 13	181 ± 29	663
		V_C (cm^3)	172 ± 24	346 ± 40	69 ± 10	160 ± 31	575
	Pooled (n=12)	$V_{\%NC}$ (%)	8.9 ± 9.5	10.4 ± 14.1	9.5 ± 10.8	8.3 ± 10.5	9.3

[a] Y: young; O: older; :M: male; F: female.
[b] DF: dorsiflexors; SO: soleus; GL: gastrocnemius (lateral head); GM: gastrocnemius (medial head).
[c] Total triceps surae (TS) volumes (SO+GL+GM); average triceps surae values reported for $V_{\%NC}$.
[d] Non-contractile volume expressed as a percentage of V_T.
[†] For absolute volume V: main effects of age (p=.014; F=6.2), gender (p<.001; F=41.5), muscle (p<.001; F=226), and volume type (V_T or V_C, p<.001; F=13.8); interaction between age and volume type (p=.039; F=4.3); for relative volume $V_{\%NC}$: main effect of age for (p<.001; F=26.7). n: number of subjects.

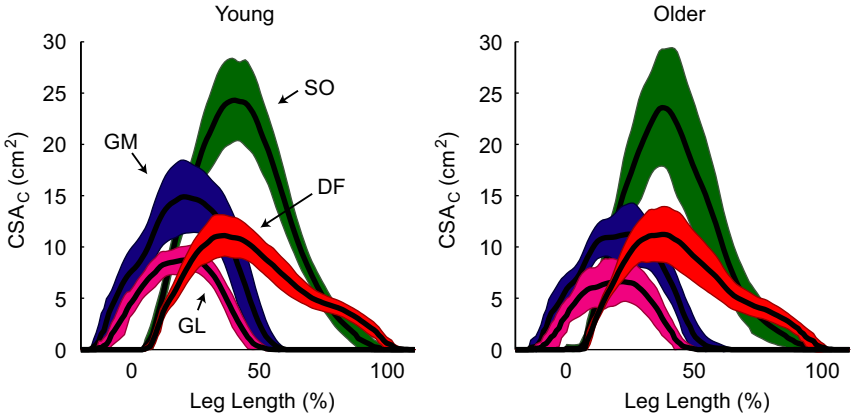

Fig. 2. Mean ± SD contractile cross-sectional areas (CSA_C) in relation to leg length (0%=knee; 100%=ankle) for each age group. DF: dorsiflexors (red); SO: soleus (green); GM: gastrocnemius (medial head; blue); GL: gastrocnemius (lateral head; magenta). (For interpretation of the references to color in this figure legend, the reader is referred to the web version of this article.)

Table 3
Parameters for generalized extreme value distributions (GEVs), which give the normalized contractile cross-sectional area (CSA_N) as a function of the longitudinal position within the leg. This specifies the "shape" of the muscles, and if integrated, gives a nominal volume (V_N). Models are specific to young (Y; n=12) and older (O; n=12) subjects.

	Muscle/age group [a]							
	DF		SO		GL		GM	
	Y	O	Y	O	Y	O	Y	O
Equation coefficients								
μ (horizontal shift)	53.1	50.9	47.9	45.3	23.9	23.0	26.4	26.4
σ (horizontal scale)	−25.0	−23.9	−18.2	−17.2	−14.1	−13.5	−15.7	−15.5
a (vertical scale)	−54.0	−50.5	−43.6	−39.4	−36.7	−34.7	−42.3	−39.4
ξ (shape)	−0.541	−0.553	−0.410	−0.426	−0.277	−0.294	−0.216	−0.284
Other parameters								
Range [p, d] [b]	[6,102]	[8,100]	[5,94]	[6,94]	[−13,52]	[−12,49]	[−15,57]	[−14,60]
Max. CSA location (%) [c]	38	35	39	37	20	19	23	21
V_N [d]	52.7	49.5	43.4	39.4	36.0	34.1	41.1	38.9
r^2 [e]	.99	.99	.99	.99	.98	.97	.98	.98

[a] DF: dorsiflexors; SO: soleus; GM: gastrocnemius (medial head); GL: gastrocnemius (lateral head); Y: young; O: older.
[b] Minimum [p] and maximum [d] slice locations, as a percentage of the leg length (0%=knee, 100%=ankle), for which the equation applies.
[c] Longitudinal location (% leg length) of the maximum contractile CSA.
[d] Nominal contractile volume (V_N) given by Eq. (3) (see text).
[e] r^2 is the coefficient of determination (variance accounted for by the equation).

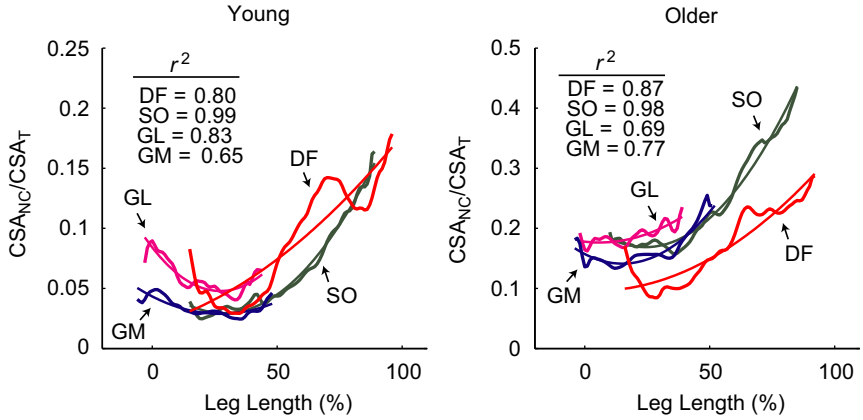

Fig. 3. Average non-contractile tissue cross-sectional area (CSA_{NC}) as a function of leg length (0%=knee; 100%=ankle), normalized to the total area (CSA_T). Data would be horizontal if the proportion of non-contractile tissue was constant along the leg (the most proximal and distal 10% of the data are not included because the much smaller CSA_T distorts the curve shapes). DF: dorsiflexors; SO: soleus; GM: gastrocnemius (medial head); GL: gastrocnemius (lateral head). Note differences in *y*-axis scaling.

Table 4
Statistics for measured (V_C) vs. predicted ($\tilde{V}_C$) contractile volumes when using a single contractile cross-sectional area (CSA_C) measurement per muscle, either near the maximum CSA_C, or at a fixed location at 30% of subjects leg length. Results are presented using equations specific to the age groups (*S*), and a non-specific equation obtained by averaging the individual group fits (*G*).

Age [a]	Eq. [b]	Measure [c]	Muscle [d]/slice location [e]							
			DF		SO		GL		GM	
			Max	30%	Max	30%	Max	30%	Max	30%
Y (n=12)	*S*	r^2	.97	.96	.87	.84	.80	.77	.85	.90
		SEE (%)	4.0	4.8	6.4	7.4	8.7	11	11	7.6
		Bias (%)	1.6	2.8	−0.1	−2.0	−5.5	7.7	−2.1	−1.1
		1.96 SD (cm^3)	17	21	49	57	22	25	49	41
	G	r^2	.97	.96	.87	.84	.80	.77	.85	.90
		SEE (%)	3.7	4.3	5.9	6.1	8.5	8.2	10.3	6.8
		Bias (%)	−6.5	−9.3	−7.5	−20	−7.8	−18	−4.7	−12
		1.96 SD (cm^3)	17	19	45	48	22	24	49	47
O (n=12)	*S*	r^2	.96	.97	.92	.72	.90	.93	.88	.86
		SEE (%)	6.4	4.8	9.2	15	12	13	8.0	10
		Bias (%)	3.9	2.4	3.6	−3.6	−4.6	12	−6.0	2.9
		1.96 SD (cm^3)	30	19	63	110	20	23	27	34
	G	r^2	.96	.97	.92	.72	.90	.93	.88	.85
		SEE (%)	6.1	4.5	9.1	13	12	9.1	8.1	9.0
		Bias (%)	−0.8	−3.4	0.5	−12	−3.4	−18	−5.6	−9.6
		1.96 SD (cm^3)	27	19	61	110	20	18	27	30

[a] Y: young; O: older.
[b] *S*: specific equation; *G*: general equation.
[c] r^2: coefficient of determination (variance accounted for by the equation); SEE: standard error of the estimate; Bias: average difference between actual and predicted contractile volumes, expressed as a percentage of the true mean; SD: standard deviation of the difference - the limits of agreement are given by: [Bias − 1.96 SD, Bias + 1.96 SD].
[d] DF: dorsiflexors; SO: soleus; GM: gastrocnemius (medial head); GL: gastrocnemius (lateral head).
[e] Max: slice location close to the maximum CSA_C (40% leg length for DF & SO; 20% leg length for GL & GM) *n*: number of subjects.

and smallest SEE. Accuracies were greater for young compared to older subjects, and were not very different for specific and general equations. The Bland–Altman analysis indicated that prediction bias (mean difference between the actual and predicted volumes) was greater for the older group (mean absolute bias=15%; specific equations) compared to young (3%; specific equations). Compared to the 30% L_{Leg} estimates, using single slices near muscle CSA_{Max} improved accuracy and bias in some cases (e.g. young DF, SO), but not in others (e.g. old DF, young GM).

Predictions were also made using CSA_{Max} estimates from three, five, and ten slices per muscle, which in general improved accuracies and biases compared to the single-slice estimates (Table 5; Fig. 4). For example, using age-specific equations and five slices gave SEE values ranging from 2–4% for young (mean across muscles=3%) and 3–7% for old (mean=4%), with an average bias of 5% and 3% for young and older subjects, respectively. Increasing the number of slices per muscle (from three to five to ten) did not result in substantial improvements, except for the GL, which had a much smaller SEE when using ten slices compared to the three-slice estimate. As for the single-slice estimates, multi-slice accuracies did not differ much between specific and general equations. The strength of the relationships (r^2) were similar between the young and older subject groups, although error (SEE) was smaller for young compared to older subjects.

4. Discussion

This study showed that the percentage of non-contractile tissue in older adults was on average 2–5 times greater than younger

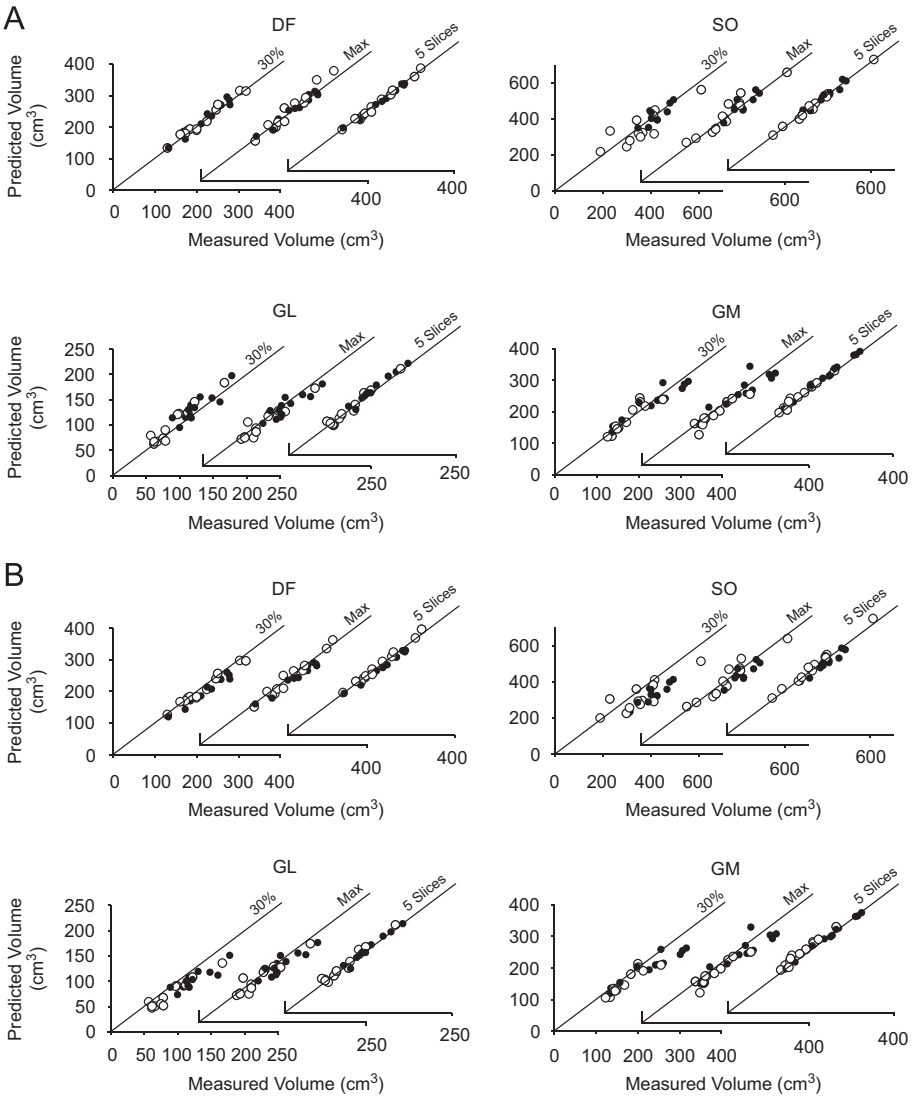

Fig. 4. Comparison between measured and predicted contractile volumes using either (A) equations that were fit to the specific age groups, or (B) general equations obtained by averaging the coefficients for the specific equations. The data for 12 young (solid symbols) and 12 older (open symbols) subjects are shown in each plot. Muscles include dorsiflexors (DF), soleus (SO), lateral head of gastrocnemius (GL) and medial head of gastrocnemius (GM). Predictions shown were based on: (1) one magnetic resonance image at 30% of the leg length (“30%”), (2) one image near the maximum contractile cross-sectional area (“Max”) for each muscle, and (3) five images for each muscle evenly distributed around the maximal cross-sectional area (“5 Slices”).

adults for the dorsiflexors (DF) and individual plantar flexors (PF), with PF towards the higher end of this range. Non-contractile tissue was distributed nonlinearly along the leg, increasing distally with minimums near the maximum compartment CSA. After fitting the CSA data with equations, single-slice CSA measures predicted contractile volume with an average error of about 8–11% for young and older adults. Using multiple slices (3–10) improved volume estimates by roughly 50%, with average errors of about 3–4%.

4.1. Age-related differences in contractile and non-contractile volumes

Contractile (V_C) and non-contractile ($V_{\%NC}$) volumes were quantified using full longitudinal sets of axial MRI images. For DF, older adults had smaller V_C and double the $V_{\%NC}$ compared to young adults, agreeing with Kent-Braun et al. (2000) and McNeil et al. (2007) who used single MRI cross-sections at maximum CSA. For PF, V_C was 22% smaller in older compared to young males, close to the 19% difference in Thom et al. (2005) but lower than the 30% difference reported by Rice et al. (1989). The discrepancy with the latter study could be due to differences in subject populations, number of slices analyzed, and imaging technology. The Rice et al. study had a larger age range for the older group (up to 90 yrs), used a single scan at maximum limb girth, and used computed tomography, which cannot distinguish muscle from tendon (Rice et al., 1989).

We know of no previous comparisons of young and older PF V_C in females, but found an 18% age-related reduction. Older PF $V_{\%NC}$ was on average four times greater than younger adults, consistent with Rice et al. (1989). In general, for the same leg volume, greater $V_{\%NC}$ reflects less contractile material. While both PF and DF play important roles in many activities of daily living (Winegard et al., 1996), the 4-fold greater PF $V_{\%NC}$ in older adults may make a larger contribution to age-related decrements in ankle function compared to the weaker DF and its smaller 2-fold difference in $V_{\%NC}$.

4.2. Contractile and non-contractile tissue distribution

We obtained measurements of longitudinal CSA distribution for DF, SO, GM, and GL muscles in young and older adults.

Table 5
Statistics for measured (V_C) vs. predicted ($\tilde{V}_C$) contractile volumes when using multiple slices (m) per muscle. Results are presented using equations specific to the age groups (S), and a non-specific equation obtained by averaging the individual group fits (G).

Age [a]	Eq. [b]	Measure [c]	Muscle [d]/Number of Slices [e]											
			DF			SO			GL			GM		
			$m=3$	$m=5$	$m=10$	$m=3$	$m=5$	$m=10$	$m=3$	$m=5$	$m=10$	$m=3$	$m=5$	$m=10$
Y ($n=12$)	S	r^2	.99	.99	.99	.93	.95	.96	.90	.97	.98	.99	.99	.99
		SEE (%)	2.2	1.8	1.7	3.8	3.6	3.5	8.1	3.9	3.4	3.6	2.0	2.6
		Bias (%)	−3.0	−1.8	−1.0	0.6	0.3	0.3	2.4	3.6	4.0	5.0	3.5	2.2
		1.96 SD (cm^3)	9.0	8.0	8.0	31	27	26	19	9.0	8.0	21	9.0	12
	G	r^2	.99	.99	.99	.93	.95	.96	.90	.97	.98	.99	.99	.99
		SEE (%)	2.2	1.8	1.7	3.6	3.4	3.3	7.9	3.8	3.3	3.5	1.9	2.5
		Bias (%)	−5.9	−4.8	−3.9	−4.1	−4.4	−4.4	0.0	1.2	1.6	2.1	0.6	−0.6
		1.96 SD (cm^3)	9.5	8.6	8.7	32	27	25	19	8.8	7.6	18	8.7	14
O ($n=12$)	S	r^2	.98	.99	.99	.99	.99	.98	.87	.97	.99	.95	.97	.96
		SEE (%)	3.9	3.0	3.5	2.5	3.1	4.0	15	7.1	4.2	5.8	4.3	4.5
		Bias (%)	−2.4	−1.4	−0.6	0.8	−0.5	−0.5	−0.8	2.5	4.7	7.0	5.9	4.2
		1.96 SD (cm^3)	16	13	15	17	20	27	24	12	8.0	21	14	15
	G	r^2	.98	.99	.99	.99	.99	.98	.87	.97	.99	.95	.97	.96
		SEE (%)	4.0	3.1	3.6	2.6	3.2	4.2	15	7.2	4.3	6.0	4.4	4.6
		Bias (%)	0.6	1.6	2.4	5.9	4.5	4.7	1.6	4.9	7.1	10	9.1	7.4
		1.96 SD (cm^3)	16	14	17	19	24	31	25	13	9.6	22	15	15

[a] Y: young; O: older.
[b] S: specific equation; G: general equation.
[c] r^2: coefficient of determination (variance accounted for by the equation); SEE: standard error of the estimate; Bias: average difference between actual and predicted, expressed as a percentage of the true mean; SD: standard deviation of the difference - the limits of agreement are given by: [Bias − 1.96 SD, Bias + 1.96 SD].
[d] DF: dorsiflexors; SO: soleus; GM: gastrocnemius (medial head); GL: gastrocnemius (lateral head).
[e] Volumes estimated using average CSA_{Max}, based on several evenly spaced CSA_C measurements, using either $m=3$, 5, or 10 slices for each muscle in the range of 30–50% of leg length for DF and SO, and 10–30% of leg length for GL and GM n: number of subjects.

Generalized extreme value (GEV) functions were used to accurately characterize age group contractile CSA_C distributions ($r^2 > .97$). The maximum CSA_C for the GL and GM was at ~20% L_{Leg}, but was more distal for the DF and SO (~40% L_{Leg}). Although Morse et al. (2005) presented data on longitudinal GL CSA_C distribution in young and old males, these data were not normalized to leg length or characterized in equation form, making comparisons with our data difficult.

A unique finding was that the proportion of non-contractile tissue (CSA_{NC}/CSA_T) was not uniformly distributed along the length of the muscles. The lowest proportion was near the maximum CSA_C, generally increasing in proximal and distal directions. Such patterns are consistent with roughly constant *absolute* amounts of non-contractile tissue along the muscle length, making the relative proportion greater as the muscles taper to their origins/insertions. The variance explained by second order polynomial fitting differed between the muscles, with the greatest r^2 (~.98) for SO, while other muscles varied with r^2 values between .65 and .87. The better fit for SO could be related to its large volume, minimizing the influence of measurement error due to CSA rounding for partially filled pixels (Elliott et al., 1997).

4.3. Prediction of contractile volume from single MRI cross-sections

The GEV model CSA_C distributions for the DF and PF muscles allow prediction of muscle volumes using CSA_C from a single MRI slice. The results showed that single-slice volume estimates had moderate accuracy for young and older subjects, with average errors of 8% (young) and 11% (old). Average biases were larger in older subjects compared to young (15% vs. 3%). Overall, the single-slice accuracies are consistent with Morse et al. (2007), who showed that a single MRI scan at 60% of femur length gave quadriceps volume estimates with ~10% error. The present study extends these findings to the DF and PF muscles, and to older individuals. However, better results for both age groups were obtained using multiple slices per muscle, reducing average prediction errors to 3–4% with 3–5% bias. Accuracies did not differ much for predictions from three, five, or ten slices, except for the GL. The use of multiple slices mitigates single-slice measurement error, and also suggests the limits of accuracy using the GEV model-based predictions. Variability in non-contractile tissue distribution may have contributed to prediction errors.

4.4. Implications for musculoskeletal modeling

This study has shown how muscle volumes can be estimated from relatively few MRI slices in both young and older adults. Non-invasive imaging technology such as MRI permits the use of subject-specific muscle properties such as contractile volume in musculoskeletal models that are sensitive to input parameters (Scovil and Ronsky, 2006). The ability to create more accurate subject-specific models of the senescent human musculoskeletal system will become increasingly useful for advancing our understanding of the functional impact of sarcopenia and other age-related muscle changes.

Conflict of interest statement

We wish to confirm that there are no known conflicts of interest associated with this publication and there has been no significant financial support for this work that could have influenced its outcome.

Acknowledgments

The authors thank Luis Rosado, Ross Miller, and Scott Caldwell for assistance with data collection and analysis, John Buonaccorsi for statistical help, and Pawel Skudlarski and Steve Foulis for MRI software help. This research was supported by the NIH Grant R03AG026281 (GEC).

Appendix A. Supplementary material

Supplementary data associated with this article can be found in the online version at doi:10.1016/j.jbiomech.2011.05.031.

References

Ackerman, M.J., 1991. The visible human project. Journal of Biocommunication 18, 14.

Anderson, F.C., Pandy, M.G., 2001. Dynamic optimization of human walking. Journal of Biomechanical Engineering 123, 381–390.

Bland, J.M., Altman, D.G., 1986. Statistical methods for assessing agreement between two methods of clinical measurement. The Lancet 327, 307–310.

Caldwell, G., Chapman, A., 1991. The general distribution problem: a physiological solution which includes antagonism. Human Movement Science 10, 355–392.

Elliott, M., Walter, G., Gulish, H., Sadi, A., Lawson, D., Jaffe, W., Insko, E., Leigh, J., Vandenborne, K., 1997. Volumetric measurement of human calf muscle from magnetic resonance imaging. Magnetic Resonance Materials in Physics, Biology and Medicine 5, 93–98.

Forsberg, A.M., Nilsson, E., Werneman, J., Bergström, J., Hultman, E., 1991. Muscle composition in relation to age and sex. Clinical Science 81, 249–256.

Gomberg, B.R., Saha, P.K., Wehrli, F.W., 2005. Method for cortical bone structural analysis from magnetic resonance images. Academic Radiology 12, 1320–1332.

Harvill, L.M., 1991. Standard error of measurement. Educational Measurement: Issues and Practice 10, 33–41.

Jubrias, S.A., Odderson, I.R., Esselman, P.C., Conley, K.E., 1997. Decline in isokinetic force with age: muscle cross-sectional area and specific force. Pflügers Archiv: European Journal of Physiology 434, 246–253.

Kent-Braun, J.A., Ng, A.V., Young, K., 2000. Skeletal muscle contractile and noncontractile components in young and older women and men. Journal of Applied Physiology 88, 662–668.

Kotz, S., Nadarajah, S., 2000. Extreme Value Distributions: Theory and Applications. Imperial College Press, London.

Kuo, A.D., Zajac, F.E., 1993. A biomechanical analysis of muscle strength as a limiting factor in standing posture. Journal of Biomechanics 26 (Suppl. 1), 137–150.

Lexell, J., Taylor, C., 1989. Variability in muscle fibre areas in whole human quadriceps muscle. How much and why? Acta Physiologica Scandinavica 136, 561–568.

McNeil, C.J., Vandervoort, A.A., Rice, C.L., 2007. Peripheral impairments cause a progressive age-related loss of strength and velocity-dependent power in the dorsiflexors. Journal of Applied Physiology 102, 1962–1968.

Mitsiopoulos, N., Baumgartner, R.N., Heymsfield, S.B., Lyons, W., Gallagher, D., Ross, R., 1998. Cadaver validation of skeletal muscle measurement by magnetic resonance imaging and computerized tomography. Journal of Applied Physiology 85, 115–122.

Morse, C., Thom, J., Reeves, N., Birch, K., Narici, M., 2005. In vivo physiological cross-sectional area and specific force are reduced in the gastrocnemius of elderly men. Journal of Applied Physiology 99, 1050–1055.

Morse, C.I., Degens, H., Jones, D.A., 2007. The validity of estimating quadriceps volume from single MRI cross-sections in young men. European Journal of Applied Physiology 100, 267–274.

Narici, M., Landoni, L., Minetti, A., 1992. Assessment of human knee extensor muscles stress from in vivo physiological cross-sectional area and strength measurements. European Journal of Applied Physiology and Occupational Physiology 65, 438–444.

Overend, T.J., Cunningham, D.A., Paterson, D.H., Lefcoe, M.S., 1992. Thigh composition in young and elderly men determined by computed tomography. Clinical Physiology 12, 629–640.

Rice, C.L., Cunningham, D.A., Paterson, D.H., Lefcoe, M.S., 1989. Arm and leg composition determined by computed tomography in young and elderly men. Clinical Physiology 9, 207–220.

Roubenoff, R., Hughes, V.A., 2000. Sarcopenia: current concepts. Journals of Gerontology Series A: Biological Sciences and Medical Sciences 55, M716–M724.

Scovil, C.Y., Ronsky, J.L., 2006. Sensitivity of a Hill-based muscle model to perturbations in model parameters. Journal of Biomechanics 39, 2055–2063.

Shrout, P.E., Fleiss, J.L., 1979. Intraclass correlations: uses in assessing rater reliability. Psychological Bulletin 86, 420–428.

Thom, J.M., Morse, C.I., Birch, K.M., Narici, M.V., 2005. Triceps surae muscle power, volume, and quality in older versus younger healthy men. Journals of Gerontology Series A: Biological Sciences and Medical Sciences 60, 1111–1117.

van Soest, A.J., Bobbert, M.F., 1993. The contribution of muscle properties in the control of explosive movements. Biological Cybernetics 69, 195–204.

Weir, J.P., 2005. Quantifying test-retest reliability using the intraclass correlation coefficient and the SEM. Journal of Strength and Conditioning Research 19, 231–240.

Winegard, K.J., Hicks, A.L., Sale, D.G., Vandervoort, A.A., 1996. A 12-year follow-up study of ankle muscle function in older adults. Journals of Gerontology Series A: Biological Sciences and Medical Sciences 51, B202–B207.

Yamaguchi, G., Moran, D., Si, J., 1995. A computationally efficient method for solving the redundant problem in biomechanics. Journal of Biomechanics 28, 999–1005.